Preprint of article appearing in Mechanics of Materials vol 40 (12) p 975-981 and available at doi:10.1016/j.mechmat.2008.07.003

An analytical solution for the load distribution along a fibre in a nonwoven network

Warren Batchelor
Australian Pulp and Paper Institute, Department of Chemical Engineering, PO Box 36, Monash University, 3800 Victoria Australia
Email: warren.batchelor@eng.monash.edu.au
+61 3 9905 3452/ Fax: +61 3 9905 3413

Abstract
This paper develops a method to analyse the load distribution along a half fibre in a non-woven or fibre composite where force is transferred into the fibre at any set of discrete contacts. The force transferred at each contact is assumed to be proportional to the displacement of the contact relative to the applied strain field. The constant of proportionality between displacement and force can be set independently for each contact. The cross-sectional area and elastic modulus of each segment between contacts can also be set independently. It was shown that the displacement, due to the applied strain, at each contact could be expressed in terms of the displacement at the last contact at the end of the fibre. As the displacement at the last contact was the sum of the previous contacts, each multiplied by a stress transfer coefficient, the stress distribution along the fibre could be solved analytically. The debonding of fibres from a paper sheet under load was simulated. The fibre load-network strain curve was found to be highly sensitive to the configuration of the crossing points. The method of analysis has application to nonwoven networks such as paper as well as nonwoven fibre composites.

Keywords
Short-fibre composites; Mechanical properties; Modelling; Stress transfer; shear-lag model; Cellulosic fibres

Preprint of article appearing in Mechanics of Materials vol 40 (12) p 975-981 and available at doi:10.1016/j.mechmat.2008.07.003

Introduction

An important factor affecting the mechanical properties of a fibre network or fibre composite under load is the stress distribution along fibres in the material. This has been frequently modelled using the shear-lag theory (Nairn, 1997), due originally to Cox (Cox, 1952). The shear-lag analysis starts by considering a fibre embedded in a matrix subject to a strain, ε, in the direction of the fibre. It is assumed that the load, dF transferred into the fibre from the matrix, over a distance, *dx*, at a position, *x*, along the fibre is linearly proportional to the displacement of *x* relative to the applied strain or $dF/dx \propto (\delta_f - \delta_m)$ where δ_f and δ_m are the fibre and network displacement, respectively, relative to a reference point. For a linearly elastic fibre this expression can be integrated (Cox, 1952; Raisanen et al., 1997) to give $\varepsilon_f(x) = \varepsilon\left(1 - \cosh\left(\beta x\right)/\cosh\left(\beta L\right)\right)$, where $\varepsilon_f(x)$ is the strain at a position x along a fibre of half length, L, elastic modulus, E and cross-section, A, and β is the shear-lag parameter giving the efficiency at which the matrix transfers stress into the fibre. The coordinate system is set with $x = 0$ at the centre of the fibre.

The shear-lag model has found widespread application (see for example (Sridhar et al., 2003; Xia et al., 2002)) in research on fibre reinforced composites. It has also been used to predict the elastic modulus (Astrom et al., 1994; Page and Seth, 1980) and strength (Carlsson and Lindstrom, 2005; Feldman et al., 1996) of nonwoven fibrous networks, such as paper, although the usefulness of the approach has been disputed (Raisanen et al., 1997). Methods to calculate β for a given matrix material and fibre dimensions have been the subject of continued research (Nairn, 1997). However, a shear lag type analysis is only fully valid if one single value of β applies along the whole length of the fibre. It is also likely to be a good approximation if the variation in β is small. There are many situations where a single value of β cannot be applied. Paper, for example, is a nonwoven network composed of naturally produced fibres with wide distributions of lengths, cross-sectional dimensions and mechanical properties. Load is only transferred into a fibre at discrete points, where the fibre comes into contact with other fibres. For a given fibre, each crossing fibre's dimensions, mechanical properties, position and crossing angle will be determined according to stochastic distributions. A non-woven or woven fibre composite is another example, as the stress transferred into a fibre of interest will vary along the fibre, due to the different stress transfer characteristics of the fibre network and matrix. Finally any fibre network or fibre composite (eg cellulosic composites made of flax or cotton fibres (Eichhorn and Young, 2003)) in which stress is transferred across the ends of the fibres will also not fulfil the classic shear-lag criterion, although some theoretical approaches have been developed to deal with such cases (Clyne, 1989).

The stress-distribution along a fibre has never been solved analytically for a network where load is transferred into a fibre at some set of discrete contact points, each with an individual value of β, although it is possible to calculate using finite element models. The problem is difficult to analyse because any force transferred into the fibre both produces and is caused by displacement the contact point along the fibre,

Preprint of article appearing in Mechanics of Materials vol 40 (12) p 975-981 and available at doi:10.1016/j.mechmat.2008.07.003

relative to the applied strain. The purpose of this paper is to present an analytical method to solve this problem.

Theory

Figure 1 shows half of a fibre, which is connected to an external fibre network by i contact points. The contact points are shown in Figure 1 as fibres. This is for convenience and in fact the analysis is valid for any form of stress transfer into the fibre that is linearly coupled to the network strain in the direction of the fibre.

The fibre is assumed to be linear elastic. The centre of the fibre at $x_0 = 0$ is set as the reference point and it is assumed that the force transferred into each half of the fibre is identical and so therefore only half the fibre needs to be considered for the purposes of this calculation. A strain of ε is applied to the external network in the direction of the fibre axis. It is assumed that force is transferred into the fibre by displacements of the contact points from their equilibrium position for the applied network strain. The displacement of the j^{th} contact is designated δ_j. The forces that develop at the j^{th} contact are assumed to linearly related to δ_j by a stress transfer coefficient, β_j, such that

$$F_j = \beta_j \delta_j \tag{1}$$

The idea is illustrated in Fig. 2, which shows segment 1 of the loaded fibre from Fig. 1. This has a strain in the first segment of ε_1 which differs from the network strain, ε, displacing the crossing point from the equilibrium position by $\delta_1 = (\varepsilon_1 - \varepsilon)(x_1 - x_0)$. It should be noted here that the values of δ are always negative. That is the displacement at each point of the crossing fibre is always less than the displacement of the network, relative to the reference point. Hence the stress transfer coefficients, β, are also negative so that the force on the fibre is in the positive direction, as indicated.

The force which has produced the strain ε_1 is the sum of the forces developed at all i crossing fibres and therefore

$$\delta_1 = \frac{(x_1 - 0)}{E_1 A_1} \sum_{j=1}^{j=i} \beta_j \delta_j - \varepsilon (x_1 - 0) \tag{2}$$

where E_1 and A_1 are the elastic modulus and cross-sectional area, respectively, of segment 1. Each segment is assumed to have a constant cross-section and elastic modulus. However, one of the strengths of the method is that the elastic modulus and the cross-section can vary from segment to segment.

The displacement at the second contact is the sum of the displacement in the first and second segments which gives

Preprint of article appearing in Mechanics of Materials vol 40 (12) p 975-981 and available at doi:10.1016/j.mechmat.2008.07.003

$$\delta_2 = (x_1 - 0)\left(\frac{\sum_{j=1}^{j=i}\beta_j\delta_j}{E_1A_1} - \varepsilon\right) + (x_2 - x_1)\left(\frac{\sum_{j=2}^{j=i}\beta_j\delta_j}{E_2A_2} - \varepsilon\right) \quad (3)$$

if $E_1A_1 = E_2A_2$ then equation (3) simplifies to

$$\delta_2 = \frac{1}{EA}\left(x_1\beta_1\delta_1 + x_2\sum_{j=2}^{j=i}\beta_j\delta_j\right) - \varepsilon x_2 \quad (4)$$

It can be shown that for the $n-1^{\text{th}}$ and n^{th} contacts that

$$\delta_{n-1} = (x_1 - 0)\left(\frac{\sum_{j=1}^{j=i}\beta_j\delta_j}{E_1A_1} - \varepsilon\right) + \ldots + (x_{n-1} - x_{n-2})\left(\frac{\sum_{j=n-1}^{j=i}\beta_{n-1}\delta_{n-1}}{E_{n-1}A_{n-1}} - \varepsilon\right) \quad (5)$$

and

$$\delta_n = (x_1 - 0)\left(\frac{\sum_{j=1}^{j=i}\beta_j\delta_j}{E_1A_1} - \varepsilon\right) + \ldots + (x_{n-1} - x_{n-2})\left(\frac{\sum_{j=n-1}^{j=i}\beta_{n-1}\delta_{n-1}}{E_{n-1}A_{n-1}} - \varepsilon\right) + (x_n - x_{n-1})\left(\frac{\sum_{j=n}^{j=i}\beta_n\delta_n}{E_nA_n} - \varepsilon\right)$$

(6)

Substitution of equation (5) in equation (6) yields

$$\delta_n = \delta_{n-1} + (x_n - x_{n-1})\left(\frac{\sum_{j=n}^{j=i}\beta_n\delta_n}{E_nA_n} - \varepsilon\right) \quad (7)$$

which may be rewritten as

$$\delta_{n-1} = \delta_n - (x_n - x_{n-1})\left(\frac{\sum_{j=n}^{j=i}\beta_n\delta_n}{E_nA_n} - \varepsilon\right) \quad (8)$$

Thus δ_{i-1}, can be written in terms of δ_i; δ_{i-2} can be written in terms of δ_{i-1} and thus in terms of δ_i, and a similar chain can be developed such that each displacement can be expressed in terms of δ_i, the displacement at the final crossing nearest the fibre end. The displacements at all the fibre crossings can be expressed in terms of δ_i and as δ_i is given by

$$\delta_i = (x_1 - 0)\left(\frac{\sum_{j=1}^{j=i}\beta_j\delta_j}{E_1A_1} - \varepsilon\right) + \ldots + (x_{i-1} - x_{i-2})\left(\frac{\sum_{j=i-1}^{j=i}\beta_{i-1}\delta_{i-1}}{E_{i-1}A_{i-1}} - \varepsilon\right) + (x_i - x_{i-1})\left(\frac{\sum_{j=i}^{j=i}\beta_i\delta_i}{E_iA_i} - \varepsilon\right)$$

(9)

Preprint of article appearing in Mechanics of Materials vol 40 (12) p 975-981 and available at doi:10.1016/j.mechmat.2008.07.003

which may be expressed in shortened form as

$$\delta_i = \sum_{k=1}^{k=i} \frac{(x_k - x_{k-1})}{E_k A_k} \left(\sum_{j=k}^{j=i} \beta_j \delta_j \right) - \varepsilon x_i \tag{10}$$

then it is possible to solve this equation to determine δ_i and thus to uniquely determine the displacements at all crossings. It is also worth noting that if EA is constant along the length of the fibre, then equation (10) simplifies to

$$\delta_i = \frac{1}{EA} \left(\sum_{j=1}^{j=i} x_j \beta_j \delta_j \right) - \varepsilon x_i \tag{11}$$

To illustrate the application of the method, the equations will now be given for the relatively simple case of three points of stress transfer for a half fibre with uniform elastic modulus, E, and cross-sectional area, A. To simplify the expressions, the stress transfer coefficients will be normalised by the elastic modulus and cross sectional area such that

$$\beta'_j = \beta_j / EA \tag{12}$$

The three points for stress transfer are designated 1, 2 and 3, with point 3 being closest to the end of the fibre. From equation (8) it can be shown that

$$\delta_2 = \delta_3 + (x_3 - x_2)(\varepsilon + \beta'_3 \delta_3) \tag{13}$$

and

$$\delta_1 = \delta_3 + (x_3 - x_2)(\varepsilon + \beta'_3 \delta_3) + (x_2 - x_1)\left(\varepsilon + \left(\beta'_3 \delta_3 + \beta'_2 \left(\delta_3 + (x_3 - x_2)(\varepsilon + \beta'_3 \delta_3)\right)\right)\right) \tag{14}$$

And from equation (11) δ_3 is given by

$$\delta_3 = x_1 \beta'_1 \delta_1 + x_2 \beta'_2 \delta_2 + x_3 \beta'_3 \delta_3 - \varepsilon x_3 \tag{15}$$

Which upon substitution of equations (13) and (14) yields

$$0 = x_1 \beta'_1 \left(\delta_3 + (x_3 - x_2)(\varepsilon + \beta'_3 \delta_3) + (x_2 - x_1)\left(\varepsilon + \left(\beta'_3 \delta_3 + \beta'_2 \left(\delta_3 + (x_3 - x_2)(\varepsilon + \beta'_3 \delta_3)\right)\right)\right)\right) + x_2 \beta'_2 \left(\delta_3 + (x_3 - x_2)(\varepsilon + \beta'_3 \delta_3)\right) + x_3 \beta'_3 \delta_3 - \varepsilon x_3 - \delta_3 \tag{16}$$

The factors in equation (16) can be rearranged in the form $0 = a + b\delta_3$ which then yields one unique solution for δ_3, which can then be substituted into equations (13) and (14) to yield δ_2 and δ_1, respectively. Clearly the complexity of the analysis grows substantially with the addition of each crossing point. However this system can be rapidly solved for a reasonable number of contacts using a mathematical package with symbolic analysis capability. The calculation can be checked for consistency by summing the forces from all contacts and checking that those forces given by the calculated displacements also yield those displacements. To see how this applies in practice, consider the following simple case of a half fibre of length, L =1000 μm and a network strain, ε, of 0.03. Stress is transferred into the half fibre at 3 contacts at $(x_1, x_2, x_3) = (300\mu m, 600\mu m, 900\mu m)$ and the normalised stress transfer coefficients

Preprint of article appearing in Mechanics of Materials vol 40 (12) p 975-981 and available at doi:10.1016/j.mechmat.2008.07.003

are $\beta_1' = \beta_2' = \beta' = 10,000$. Substitution of these values in equation (16) and solving yields $\delta_3 = -216/91$ μm, from which $\delta_2 = -45/91$ μm and $\delta_1 = -9/91$ μm can be obtained. The correctness of the solution can be shown by substituting these values into equation (2) which yields $\delta_1 = x_1\left(10,000\left(\frac{216+45+9}{91}\right)10^{-6} - 0.03\right)$ which is -0.09890 μm or -9/91 μm.
The correctness of the solution is proven as equation (2) was not used as part of the derivation of equation (16).

Applications
There are three major applications for the method. The first application is in calculating the load distribution in a fibre when the stress transfer varies along the length of the fibre. This will occur in any nonwoven or nonwoven composite. It will also occur in composites where stress transfer occurs across the ends of the fibres. The second application is to model the evolution of the stress development as loading progresses towards failure and the bonds transferring the load begin to fail. The third application is to model stress transfer in non-uniform fibres, where elastic modulus and cross-sectional area vary along the fibre.

To demonstrate the first application, a system is considered with a half fibre of 1000μm length with 20 contacts, at 50μm, 100μm, 150μm…1000μm. Instead of β'=10,000 used in the previous example, β' has been generated as a random number either between 0 and 5,000 (fibres 1-3) or between 0 and 1000 (fibres 4-6). The results are shown in Figure 3 as the ratio of the local strain along the fibre to the network strain. All strain distributions are similar in shape to the classic shear-lag distribution as they are approximately constant towards the middle of the fibre at $x = 0$ and fall at an increasing rapid rate towards the end of the fibre. The strain at $x = 0$ for fibres 1-3 is essentially the same as the network strain, while fibres 4-6 with the lower stress transfer coefficient have a maximum strain of around 0.9 of the network strain. The random distribution of β' along a fibre can be observed as the fall in strain moving towards the fibre end is neither uniform, nor identical from fibre to fibre. The figure shows that strain distribution is much less dependent on the values of β' when the values of β' are higher on average.

To demonstrate the second application, the debonding of a fibre from a loaded nonwoven structure will be simulated. The non-woven taken as an example is a paper sample that comes from an investigation into factors affecting the strength of paper (He, 2005). The starting material was a never bleached, undried, laboratory cooked radiata pine kraft with a kappa number of 30. This pulp was prepared from the starting stock by double fractionation in a hydrocyclone, which altered the fibre cross-sectional shape, while keeping the fibre length essentially constant. The fibre shape was measured in the sheet using a combination of resin embedding and confocal microscopy (He et al., 2003). The fibre shape was then characterised by measuring the cross-sectional area of the irregular fibre shape and from the dimensions of the smallest rectangular bounding box that could be fitted around the fibre (He et al.,

Preprint of article appearing in Mechanics of Materials vol 40 (12) p 975-981 and available at doi:10.1016/j.mechmat.2008.07.003

2003). The summary data for the sample are shown in Table 1. The fibre cross-sectional area was assumed to be constant along the length of the fibre.

The fibre-fibre contacts in the structure were also measured by examining fibres sectioned longitudinally by the sheet cross-section (He et al., 2004) and directly counting fibres in contact. The distances between fibre contact centres, $x_n - x_{n-1}$, were measured and shown to be fitted by a two-parameter Weibull probability density function (PDF), as given by equation (17),

$$f(x_n - x_{n-1}) = \frac{c}{b}\left(\left(x_n - x_{n-1}\right)/b\right)^{c-1}\left(\exp(-\left(x_n - x_{n-1}\right)/b\right)^{c}\right) \qquad (17)$$

where b and c are constants, and $b, c > 0$, and $x_n - x_{n-1} \geq 0$. For the sample simulated here, the fitted parameters were $b = 86.1\,\mu\text{m}$ and $c = 1.43$. Each contact was assigned to be either a full or a partial contact, depending on whether the entire width of the fibre was in touch with the fibre of interest or not. Partial contacts arise because the fibres become twisted during the sheet making process. For the sample simulated here only 24% of the measured contacts were classified as full contacts. The contact positions for each fibre were randomly generated from the probability density function given in equation (17). The distance to the first contact from $x = 0$ was generated from half the value generated by initial application of equation (17), as the calculation assumes that the fibre contacts are distributed symmetrically around the middle of the fibre. The distance to the second contact was then generated from equation (17) and added to the position of the first contact. Contacts were generated in this manner until the end of the fibre was reached.

The simulations presented here examined the effect of the randomly assigned configuration of the crossing fibres. To do this, it was assumed that the stress transfer coefficient was the same for all fibre contacts at $\beta'_j = 1000$. The orientation distribution of the crossing fibres was also neglected. Instead it was assumed that each fibre crossed at the average crossing angle of $\theta_{av} = \pi/2 - 1$ (He et al., 2003). Each contact was randomly assigned to be either a full contact or a partial contact, according to the measured statistics. The area of each full contact was then assumed to be $D_w^2/\sin\theta_{av}$, where D_w is the fibre width shown in Table 1. The area of each partial contact was randomly assigned a fraction, λ, between 0 and 1 of the area of a full contact. For the purposes of this analysis, the shear bond strength of the contacts was assumed to be $\sigma_b = 10$ MPa such that the breaking load of an individual partial contact was $\lambda\sigma_b D_w^2/\sin\theta_{av}$. The possible fracture of the fibres was ignored. The elastic modulus of the fibres was assumed to be 30 GPa.

For the simulations the network strain was started at 0 and then increased in steps of 0.002 to a final strain of 0.046. For each network strain, the stress distribution along the fibre and the load at each contact was calculated. The load at an individual contact was then compared with the breaking load of the contact. If the breaking load of the contact was exceeded, then the contact was removed from the simulation and the stress distribution and load at each contact was recalculated. This cycle was

Preprint of article appearing in Mechanics of Materials vol 40 (12) p 975-981 and available at doi:10.1016/j.mechmat.2008.07.003

repeated until the load at each contact was less than the breaking load of the contact, after which the network strain was then incremented by 0.002 and the cycle repeated.

The results of the simulation are shown in detail for two fibres in Figures 4 and 5. To simplify the presentation of the figures only the simulations at strains at intervals of 0.006 have been shown. Fibre 1 (Figure 4) and fibre 2 (Figure 5) have 14 and 25 contacts, respectively. Such a wide distribution of contacts is solely due to the distribution of distances between contacts given in equation (17). The measured load distributions along the length of the fibres show similar patterns for both simulations. No bond breakage occurred for network strains of 0.006, 0.012 and 0.18 for fibre 1. If there are no bond breakages, then the load distributions will scale with the network strain, as the fibre is assumed to be linearly elastic. This is observed in Figure 4, in that the load, at any given position, calculated at a network strain of 0.18 is three times the load calculated at a network strain of 0.006. In contrast the first bond for fibre 2 was calculated as breaking at a network strain of only 0.08, despite the increased number of contacts transferring stress into the fibre. This is due to the area of this individual contact being particularly small.

It is also interesting to note that the maximum load developed at the middle of fibre 1 at a network strain of 0.006 was 0.0189N, while the corresponding maximum load for fibre 2 at the same network strain was 0.0248N. The difference between the two was entirely because the fibre 2 has far more contacts transferring load.

For fibre 1, 1 bond broke at a network strain of 0.02 and a further five bonds broke at a network strain of 0.022 and the fibre began to debond from the network, so that only the section of the half fibre between 0 and 600μm was under load at a network strain of 0.036. This debonding process was accompanied by a sharp drop in the maximum load on the fibre. For fibre two, five bonds had already broken at a network strain of 0.02 and a further five bonds broke when the network strain was increased to 0.022 and this fibre also began to debond from the network at the end.

Figure 6 shows the fibre average load for six fibres as a function of network strain, as well as the average of the six fibres. Figures 4 and 5 show the load distribution along fibres 1 and 2, respectively, from which the fibre average loads were calculated. The individual fibres, as well as the average curve, all display an initial linear region. Except for fibre 5, all fibre load-strain curves also display a yield point, occurring before the point of maximum load. This yield point corresponds to the first bond failure. The six fibres display wide variability in the maximum load attained and the strain at the point of maximum load, despite the fact that the individual fibres all have the same elastic modulus and cross-sectional area and the stress transfer coefficient at each point of contact is identical. This variability is due only to the distributions in the number and area of the contact points.

This type of analysis can be used to simulate the failure of paper and other nonwovens. This is because the failure of paper and other nonwovens is generally triggered by the failure either by fracture or by debonding of those fibres aligned with the stress direction. A number of additional factors would need to be considered in order to do develop an accurate simulation.

Preprint of article appearing in Mechanics of Materials vol 40 (12) p 975-981 and available at doi:10.1016/j.mechmat.2008.07.003

For nonwovens made of natural wood pulp fibres, variation between and along the fibres must be taken into account. Elastic modulus in wood pulp fibres varies systematically with position in the tree (Long et al., 2000) controlled by the orientation of the cellulose microfibrils with respect to the long axis of the fibre (Page et al., 1972). Random defects introduced in the pulping process also reduce the overall elastic modulus measured from single fibre tests (Page et al., 1972), as well as the elastic modulus at the location of the defect. Further defects are introduced at fibre-fibre contacts due to differential shrinkage as the fibres dry after the sheet is formed from fibres in suspension (Page and Tydeman, 1966), producing an area of lower elastic modulus with low yield stress. Individual wood fibres also have a cross-sectional area that is approximately constant in the middle of the fibre but tapers to a point at the fibre's ends (Cote, 1980). It is not known if local elastic modulus correlates in any way with local cross-sectional area.

The tapering of the cross-sectional area and variation, from segment to segment, of elastic modulus along a fibre can be readily modelled using the approach presented here, as both elastic modulus and cross-sectional area can be set independently for each segment. The method is also rapid enough to make sufficient simulations for averages of fibre properties.

One limitation of the method is that it is restricted to linear elastic fibres and the accuracy of the simulation would need to be carefully considered if significant plastic deformation of the fibres is expected.

Conclusions

A new method has been developed to calculate the force distribution on a fibre in a loaded network where force is transferred into the fibre at discrete points. The method allows for any distribution of contact points and for each contact point to have its own stress transfer coefficient. The method show great promise in analysing the failure of nonwovens and nonwoven composites.

Acknowledgements

The support of the Australian Research Council through the Large grant program is acknowledged. Dr Jihong He is acknowledged for useful discussions.

References

Astrom J., Saarinen S., Niskanen K., Kurkijarvi J., 1994. Microscopic mechanics of fiber networks. Journal of Applied Physics 75(5), 2383-2392.

Carlsson L.A., Lindstrom T., 2005. A shear-lag approach to the tensile strength of paper. Composites Science and Technology 65(2), 183-189.

Clyne T.W., 1989. A simple development of the shear lag theory appropriate for composites with a relatively small modulus mismatch. Materials Science and Engineering a-Structural Materials Properties Microstructure and Processing 122(2), 183-192.

Cote W.A., 1980. Papermaking fibers : A photomicrographic atlas Syracuse University Press, Syracuse.

Preprint of article appearing in Mechanics of Materials vol 40 (12) p 975-981 and available at doi:10.1016/j.mechmat.2008.07.003

Cox H.L., 1952. The elasticity and strength of paper and other fibrous materials. British Journal of Applied Physics 3(3), 72-79.
Eichhorn S.J., Young R.J., 2003. Deformation micromechanics of natural cellulose fibre networks and composites. Composites Science and Technology 63(9), 1225-1230.
Feldman H., Jayaraman K., Kortschot M.T., 1996. A monte carlo simulation of paper deformation and failure. J. Pulp Pap. Sci. 22(10), J386-J392.
He J., Batchelor W.J., Markowski R., Johnston R.E., 2003. A new approach for quantitative analysis of paper structure at the fibre level. Appita J. 56(5), 366-370.
He J., Batchelor W.J., Johnston R.E., 2004. A microscopic study of fibre-fibre contacts in paper. Appita J. 57(4), 292-298.
He J., 2005. Quantitative study of paper structure at the fibre level for the development of a model for the tensile strength of paper, PhD Thesis. Monash University, Melbourne.
Long J.M., Conn A.B., Batchelor W.J., Evans R., 2000. Comparison of methods to measure fibril angle in wood fibres. Appita J. 53(3), 206-209.
Nairn J.A., 1997. On the use of shear-lag methods for analysis of stress transfer unidirectional composites. Mechanics of Materials 26(2), 63-80.
Page D.H., Tydeman P.A., 1966. Physical processes occurring during the drying phase, in: Bolam F., (Ed. Consolidation of the paper web transactions of the symposium held at cambridge, september 1965. Technical Section of the British Paper and Board Makers' Association, London, pp. 371-396.
Page D.H., El-Hosseiny F., Winkler K., Bain R., 1972. The mechanical properties of single wood-pulp fibres. Part i: A new approach. Pulp Paper Mag. Can. 73(8), 72-77.
Page D.H., Seth R.S., 1980. The elastic modulus of paper ii. The importance of fiber modulus, bonding, and fiber length. Tappi 63(6), 113-116.
Raisanen V.I., Alava M.J., Niskanen K.J., Nieminen R.M., 1997. Does the shear-lag model apply to random fiber networks. Journal of Materials Research 12(10), 2725-2732.
Sridhar N., Yang Q.D., Cox B.N., 2003. Slip, stick, and reverse slip characteristics during dynamic fibre pullout. Journal of the Mechanics and Physics of Solids 51(7), 1215-1241.
Xia Z., Okabe T., Curtin W.A., 2002. Shear-lag versus finite element models for stress transfer in fiber-reinforced composites. Composites Science and Technology 62(9), 1141-1149.

Preprint of article appearing in Mechanics of Materials vol 40 (12) p 975-981 and available at doi:10.1016/j.mechmat.2008.07.003

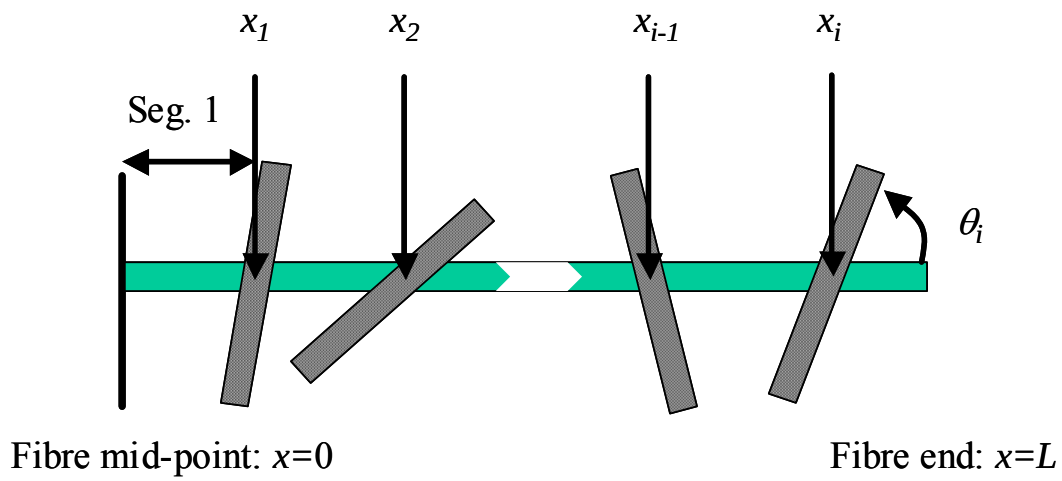

Figure 1 Unstrained half fibre of length, L, with i crossing fibres.

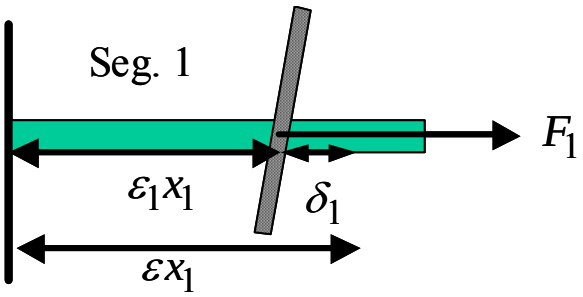

Figure 2. Displacement of the first crossing point from equilibrium position in the applied strain field, ε.

Preprint of article appearing in Mechanics of Materials vol 40 (12) p 975-981 and available at doi:10.1016/j.mechmat.2008.07.003

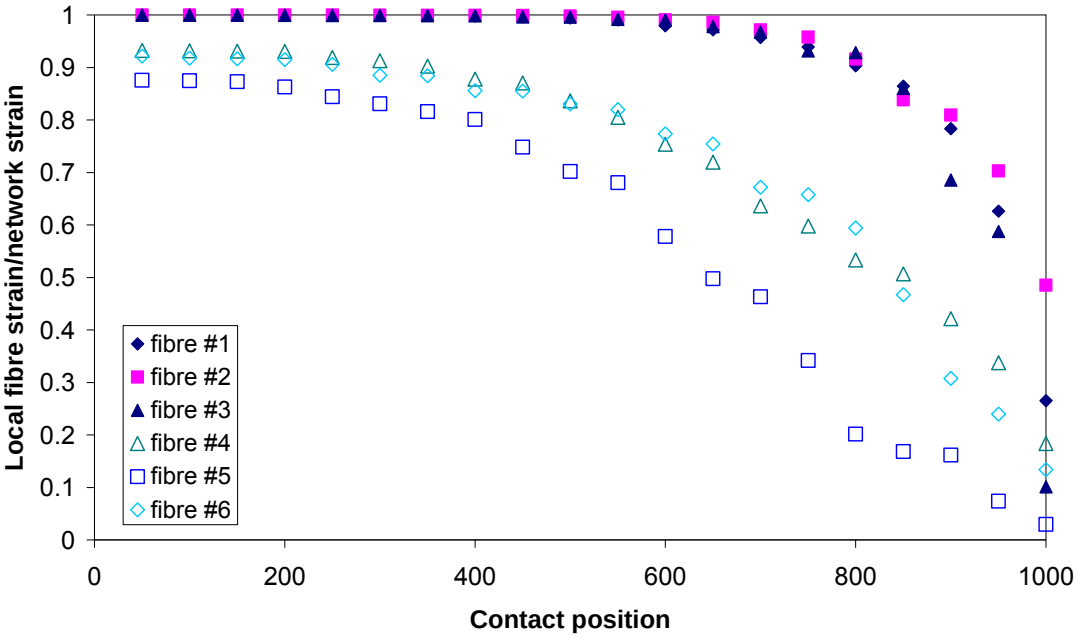

Figure 3. Calculated stress distributions for six fibres. Fibres 1-3 have β'_j for each contact having a random value between 0 and 10,000. Fibres 4-6 have β'_j for each contact having a random value between 0 and 1,000.

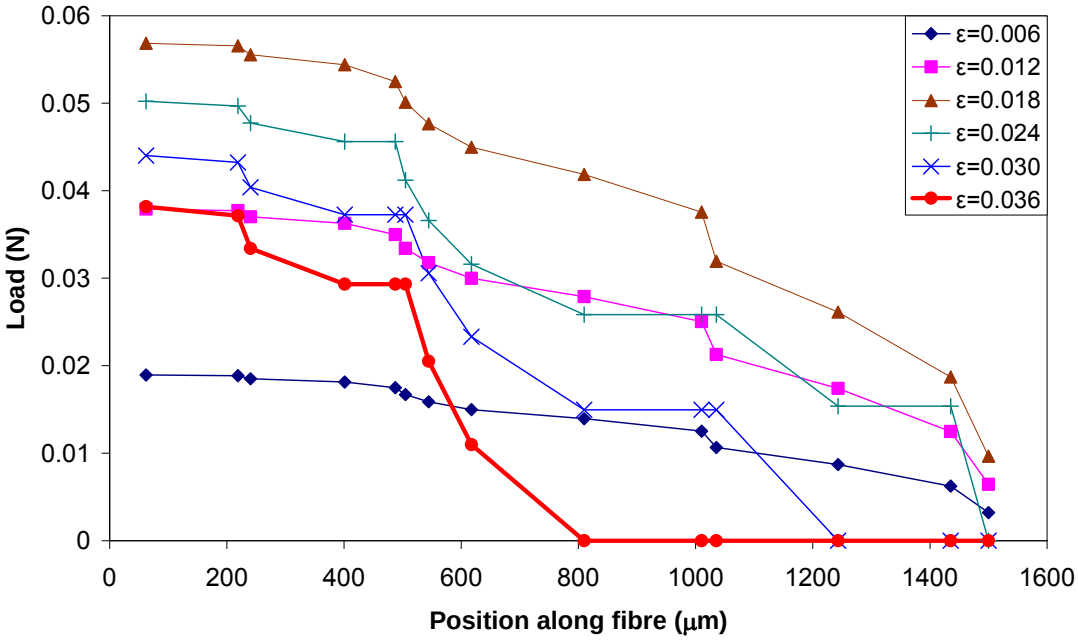

Figure 4. Load distribution along fibre 1 with $\beta'_j = 1000$ and fibre and fibre network statistics given in Table 1. The legend indicates the overall network strain along the length of the fibre.

Preprint of article appearing in Mechanics of Materials vol 40 (12) p 975-981 and available at doi:10.1016/j.mechmat.2008.07.003

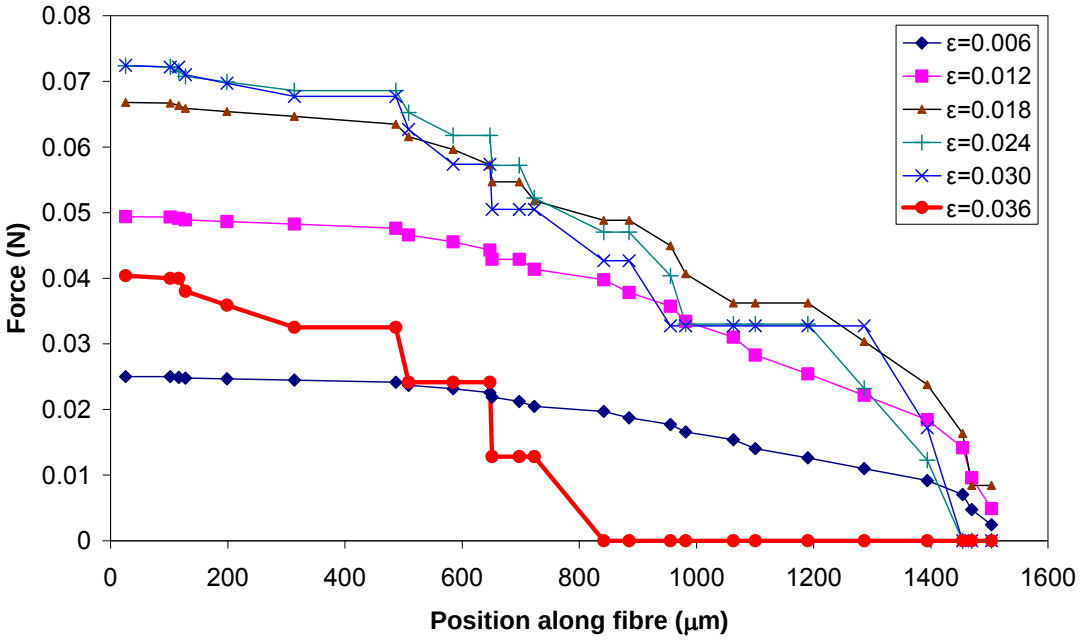

Figure 5. Load distribution along fibre 2 with $\beta_j' = 1000$ and fibre and fibre network statistics given in Table 1. The legend indicates the overall network strain along the length of the fibre.

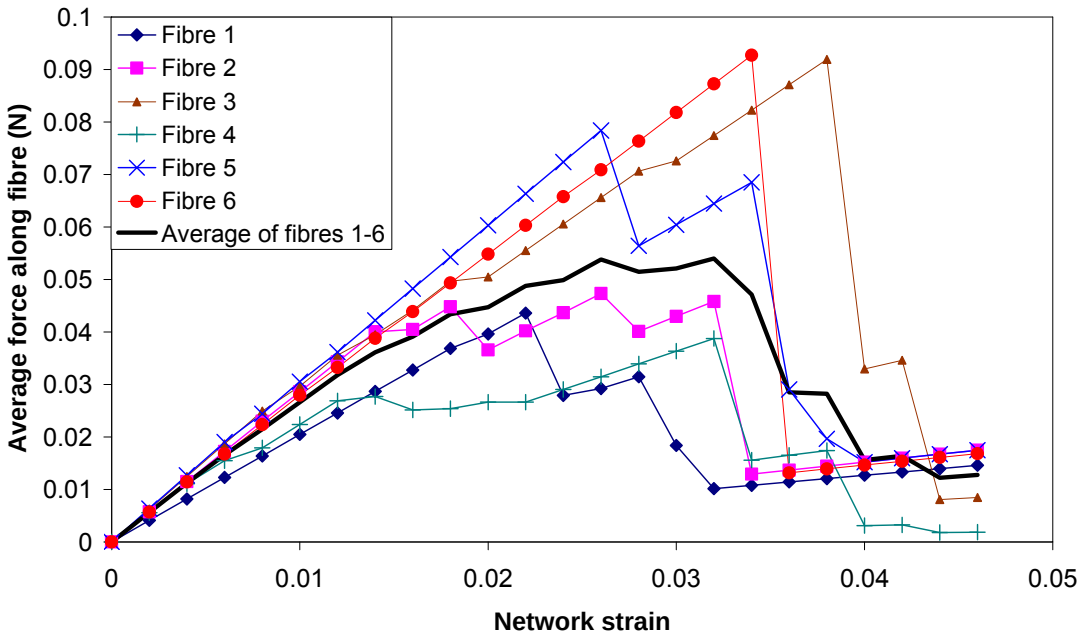

Figure 6. Simulations of average force along the fibre versus network strain for six fibres.

Preprint of article appearing in Mechanics of Materials vol 40 (12) p 975-981 and available at doi:10.1016/j.mechmat.2008.07.003

Table 1 Fibre and sheet parameters for the material used in the simulations.

Pulp	**Hydrocyclone Fraction**	**Sheet Pressing level**
Radiata pine, Kappa number of 30	Reject	0 MPa
Fibre height (μm)	**Fibre width (μm)**	**Fibre wall area (μm^2)**
16.45 ± 0.93	30.19 ± 1.35	192 ± 10
Fibre length	**No. of full contacts per fibre (average)**	**No. of partial contacts per fibre (average)**
3.34 mm	10.6	32.9
Sheet apparent density (kg/m^3)	**Length weighted Fibre length (mm)**	
218	3.14	